Genetic manipulation of structural colour in bacterial colonies

Villads Egede Johansen[a,1], **Laura Catón**[b,1], **Raditijo Hamidjaja**[b], **Els Oosterink**[c], **Bodo D. Wilts**[d,e], **Torben Sølbeck Rasmussen**[f], **Michael Mario Sherlock**[a], **Colin J. Ingham**[b,2], and **Silvia Vignolini**[a,2]

[a]University of Cambridge, Department of Chemistry, Lensfield Road, Cambridge, CB2 1EW, United Kingdom; [b]Hoekmine BV, Room 1.091 (iLab), Kenniscentrum Technologie en Innovatie, Hogeschool Utrecht, Heidelberglaan 7, 3584 CS, Utrecht, The Netherlands; [c]Wageningen Food & Biobased Research, Bornse Weilanden 9, 6708 WG, Wageningen, The Netherlands; [d]Department of Physics, University of Cambridge, JJ Thomson Avenue, CB3 0HE, Cambridge, United Kingdom; [e]Adolphe Merkle Institute, University of Fribourg, Chemin des Verdiers 4, CH-1700 Fribourg, Switzerland; [f]Department of Biotechnology and Biomedicine – Infection Microbiology, Technical University of Denmark, Anker Engelunds Vej, Building 301, 2800 Kgs. Lyngby, Denmark

Naturally occurring photonic structures are responsible for the bright and vivid coloration in a large variety of living organisms. Despite efforts to understand their biological functions, development and complex optical response, little is known of the underlying genes involved in the development of these nanostructures in any domain of life. Here, we used *Flavobacterium* colonies as a model system to demonstrate that genes responsible for gliding motility, cell shape, the stringent response and tRNA modification contribute to the optical appearance of the colony. By structural and optical analysis, we obtained a detailed correlation of how genetic modifications alter structural colour in bacterial colonies. Understanding of genotype and phenotype relations in this system opens the way to genetic engineering of on-demand living optical materials, for use as paints and living sensors.

Genetics | Structural colour | Flavobacteria | Self-organisation | Disorder

Besides pigmentation, nature's palette comprises colours that can be achieved by nano-structuring materials at the scale of visible light wavelengths. In this way, living organisms are able to modify their optical appearance (in terms of colour and angular dependency) with a large degree of freedom (1–3). As an example, while vivid, iridescent colours are obtained from light interacting with periodically arranged scattering elements, less angle-dependent colours rely on quasi-ordered (4) or completely random structures (5, 6). Such structural colours are found in a large variety of organisms spanning all kingdoms of life, from eukaryotes (1, 3, 7) to prokaryotes (8, 9). In many species, the biological significance of structural colouration represents an evolutionary advantage for camouflage (10), sexual selection (11), thermal regulation (12), photosynthesis (13, 14) and intra-species signalling (15, 16). Despite such variety of mechanisms and species displaying structural colouration, there is still little knowledge on the processes regulating the development of such colours in any living system (17–20) in terms of genotype-phenotype relation, which is key to the understanding of development, function and evolution of structural colours (21).

In this work, *Flavobacterium* strain IR1 was used as a model system. *Flavobacteria* are widely distributed, Gram-negative, biopolymer-degrading bacteria. Their motility is via gliding, where cells move over a surface in a pili-independent, flagella-independent manner using the proton motive force to generate traction via a novel molecular motor (22). IR1 colonies display vivid, bright structural colouration, similar to the gliding bacteria from other Cytophaga-Flavobacterium-Bacteroides phylum (8, 9, 23). Through transposon insertions in the WT strain, thus creating a library of genetic variants with non-

essential genes knocked out, we were able to select mutants displaying different optical properties and subsequently map the genes responsible against the sequenced IR1 genome. The structural and optical characterisation of wild type and mutant colonies were combined with a genetic study of the pathways responsible for the spatial organisation of the bacteria. This coordinated study of genotype-phenotype relation provides an unparalleled insight into the genetic pathways responsible of structural colours from living organisms. Furthermore, by analysing the development of structural colours in different growing conditions and substrates (including algae and other biotic surfaces) we suggest where bacterial colonies may exhibit structural colour in their natural environment.

Overview of novel *Flavobacterium* strain and mutants

The bacterial strain IR1 was isolated during a screening of estuarine sediment samples from the Neckarhaven region of Rotterdam harbour (NL). The cultured strains of *Flavobacteria* most closely related to IR1 were *Flavobacterium aquidurense* and *Flavobacterium pectinovorum* with 99% identity on the

---

Significance Statement

We demonstrate the first genetic modification of structural colour in any living system by using bacteria (IR1) as a model system. IR1 colonies consist of rod-shaped bacteria that pack in a dense hexagonal arrangement through gliding and growth, thus interfering with light to give a bright, green and glittering appearance. By generating IR1 mutants and mapping their optical properties, we show that genetic alterations can change colony organisation and thus their visual appearance. The findings provide insight into the genes controlling structural colour, which is important for evolutionary studies and for understanding biological formation at the nanoscale. At the same time, it is an important step towards directed engineering of photonic systems from living organisms.

---

www.pnas.org/cgi/doi/10.1073/pnas.XXXXXXXXXX

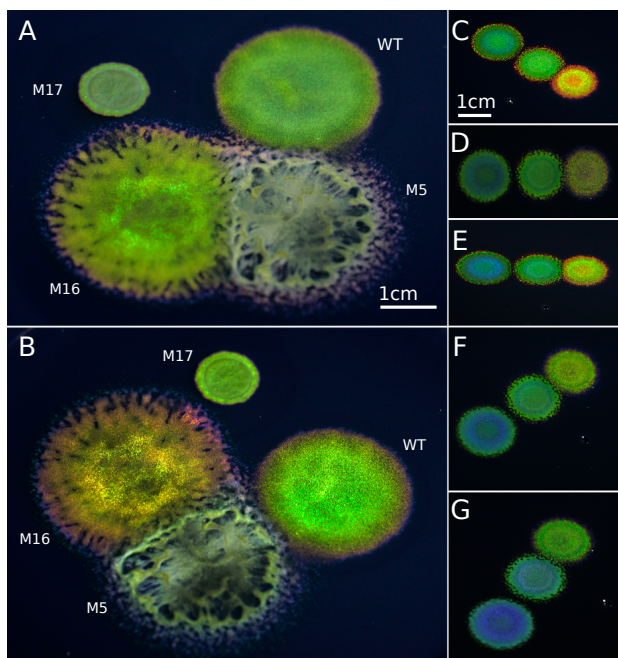PNAS | January 19, 2018 | vol. XXX | no. XX | 1–7

Fig. 1. Structural colouration of *Flavobacterium* IR1 wild type and mutants. A-B) Photographs of WT and three mutants, grown for 4 days, taken at two different angles to exhibit the colonies' pronounced angle-dependent colouration. WT and M16 produce vivid colouration whereas M17 produce some colouration and M5 very little in comparison. The scale bar in A also applies to B. C-G) Mutants M22, M65 and M41 (left to right on all photographs) photographed from five different angles under the same illumination showing the variation in colour after growth for 2 days. D is photographed from directly above, whereas the other observation angles are oblique. The scale bar in C also applies to D-G.

basis of 16S sequence comparison (see Methods and SI Appendix Fig. S1). *F. aquidurense* was originally isolated from a freshwater creek in Germany (24) and *F. pectinovorum* from soil in the United Kingdom (25). Neither bacterium has been reported to display structural colouration. On ASWBC agar plates (see SI Appendix Tables S1 and S2 for definitions), the wild type (WT) IR1 strain showed gliding motility and displayed a bright, brilliant green structural colouration as seen in Fig. 1A-B. Libraries of mutants were generated using the HiMar transposon and screened for altered optical properties. Strains with different optical properties (ranging from intense red to blue colours to mutations with reduced or no colouration) were isolated, see Fig. 1A-G. The WT strain and three mutants labelled M5, M16 and M17 were selected as representative models to study the interplay between motility, cell geometry and other aspects underpinning structural organisation of the bacterial colonies (Fig. 1A-B). M5 had comparable motility and cell shape to the WT but failed to provide clear structural colouration under the same growing conditions. Colonies of M16 had a very intense, red-shifted appearance. M17 displayed decreased motility compared to WT and a barely visible angle-dependency. An overview of the physical parameters of key mutants and the mapping of transposon insertions leading to these phenotypes is provided in SI Appendix Table S3.

Differences in organisational capacity are revealed by electron microscopy

To gain insight into the structural arrangement causing the colouration, we performed structural characterisation by Scanning Electron Microscopy (SEM) on fixed colonies (Fig. 2A-D). Studies by SEM were facilitated by a fixation procedure that resulted in the dried material maintaining a structural colour (SI Appendix Fig. S10). A clear difference in bacteria cell geometry between strains was found and the trend was confirmed by statistically significant measurements of cell lengths and diameters based on several images (SI Appendix Fig. S6A-H). The WT colony had a significantly lower variation in cell diameter than the mutant colonies, which possibly facilitates the packing into a regular lattice. The length of the WT bacteria is comparable in size and variation to M5, while M16 and M17 were shorter and longer than the WT, respectively. M17, despite being significantly longer than the WT, stacked in defined layers like the WT and M16 – albeit less densely. M5, however, was not as well organised as the WT and the bacteria were poorly aligned with respect to their neighbouring cells (Fig. 2B).

The regularity of the cells within these colonies was investigated by calculating the spatial autocorrelation of the SEM images (SI Appendix Fig. S7). The profiles of the autocorrelation, shown in SI Appendix Fig. S7E-H, provided good estimations of the packing order of the bacteria. A particularly long-ranged correlation was observed in WT and M16, indicating that the relative position and orientation of bacteria were maintained over tens of microns. M5 and M17 showed little or no correlation. This difference in packing order was predicted to strongly influence the optical response of the bacterial colonies, as will be discussed later. From the autocorrelation analysis, the periodicities of the bacterial arrangements were estimated to be ~ 357 nm, ~ 527 nm and ~ 364 nm for WT, M5 and M16 respectively (see Methods and SI Appendix Fig. S7E-G). For M17 it was not possible to extract a meaningful estimate due to lack of a clear peak in the autocorrelation spectrum, indicating a lack of ability to organise in a regular pattern (SI Appendix Fig. S7L).

Photonic response of colonies are closely related to local colony organisation

The WT and selected mutants cultured on ASWBC agar were studied with an optical goniometer. Fig. 2E-H show the scattering behaviour of the different bacterial strains when illuminated at a grazing incidence angle of $-60°$ with respect to the normal of the surface, with the complete set of measurements for different incident angles reported in SI Appendix Fig. S3. For all colonies, a strong specular reflection arising from the air interface is visible at $60°$, which is mainly dominated by the reflection from the agar. We therefore focused our analysis on the scattering properties of the colonies at non-specular angles. In fact, the periodic arrangement of the bacteria dramatically affects the visual appearance of the colony. In case of perfect packing (where the bodies of the bacteria form a two-dimensional close-packed hexagonal lattice as schematically shown in Fig. 3A), the colony diffracts light only at angles specified by the grating equation (see Methods). The intensity profile of the diffracted light depends on the lattice constant and the packing geometry, resulting in
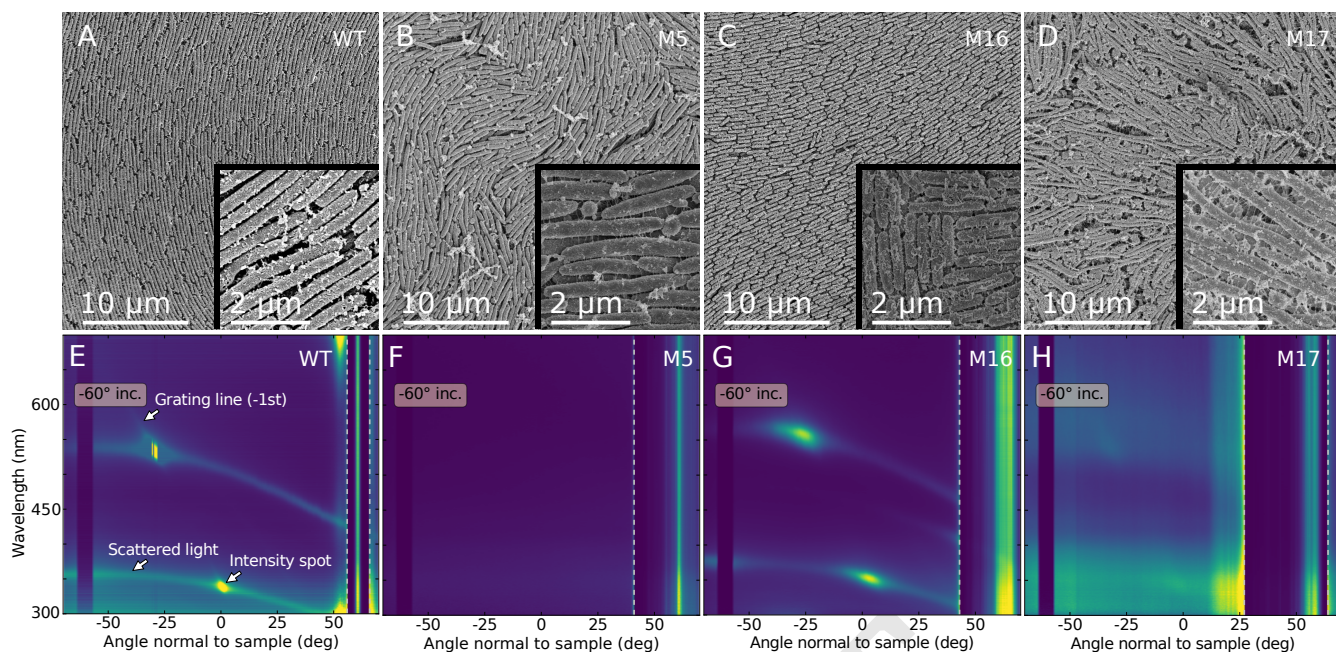
Fig. 2. Structural and optical investigations of IR1 strains. A-D) SEM top view images of the four bacterium strains ,WT, M5, M16 and M17, at identical magnifications. E-H) Scattered intensity for samples upon light illumination with an incident angle of $-60°$. In order to visualise the specular reflections, the signals within the dashed lines are divided by 900, 200, 350 and 250 respectively from left to right. In D, text annotations highlight the features caused by structural organisation: confined intensity spots lying on a very weak line governed by the grating equation (stated in Methods), as well as a more defined scattered line spanning the whole angular range and also crossing the diffraction spots. The specular reflection between dashed lines has been divided by stated factor to fit on the same colour scale.

brighter colour-selective reflections at specific angles (Fig. 3A-B). For example, the grating equation and the scale-invariance of Maxwell's equations imply that a larger lattice constant compresses the angular distribution of diffraction spots and gives longer peak reflection wavelengths.

Deviations from the ideal, periodic structure can be grouped in two categories: (i) disorder in the packing geometry, as depicted in Fig. 3C, and (ii) disorder in domains with the same orientation of bacteria, as shown in Fig. 3D. The first effect is the dominant contribution to the scattered light around the two diffraction spots at 350 nm and 530 nm in Fig. 2E. The latter effect makes the scattering signature independent of in-plane rotation (SI Appendix Fig. S4).

The diffraction spots for the WT strain are clearly distinguishable (Fig. 2E) and in agreement with the grating equation (SI Appendix Fig. S3). Their broadening in both angle and wavelength can be attributed to the variation of the bacteria diameter. Such packing gives rise to a glittering, angle-dependent appearance of the bacteria strains, as was previously observed by Kientz and co-workers (26, 27).

Strong diffraction peaks were also visible for M16, revealing a high level of order in the colony, as supported by the structural analysis. As expected, such diffraction features are less prominent in M17 and absent in M5. By using the grating equation, the lattice constant for the different strains WT, M16 and M17 can be estimated as ~ 400 nm, ~ 430 nm and ~ 400 nm, respectively (see Methods and SI Appendix Fig. S3). These values were consistent within the error margin of the SEM observations, considering the 5%-10% shrinkage that typically arises from fixation of the sample. The presence of strong diffraction peaks for WT and M16 reveals a high level of order in the colonies. In contrast, the lack of diffraction peaks in M5 indicates a poor organisation of the bacteria, see
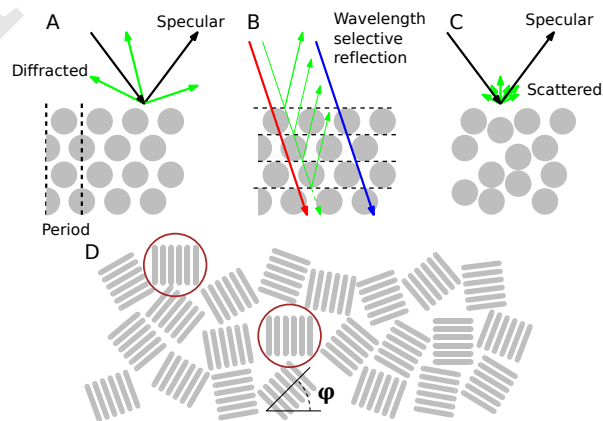

Fig. 3. Diagrams explaining the light scattering observed from colonies of IR1. A) If the cells are arranged in a strictly periodic manner, they will only reflect light at certain angles, but with a very strong intensity as described by the grating equation (see Methods). B) The intense colour selectivity is determined by the layered stacking of the bacteria, where interference for example reflects green light but transmit blue and red. C) If this periodicity is disrupted, the grating effect is obscured, and less strong intensity of reflected light is observed, but over a broader angular range. D) Top view of bacteria. Since the bacteria macroscopically do not have a preferred orientation with respect to in-plane rotation (φ), the visual appearance is independent of rotation along this axis. For example, only the two encircled, aligned areas will contribute to the optical response in the observation plane perpendicular to their orientation.

Fig. 2B, despite the presence of a certain degree of order in the autocorrelation (SI Appendix Fig. S7F). This suggests that the packing of the M5 strain in the vertical direction is not well maintained (Fig. 3C), and that the bacteria are not forming distinct layers in the colony, as is the case for the other strains (Fig. 2B). M17, on the other hand, display a weak and broad diffraction around 350 nm and 520 nm. In this case, even though the colony fails to create an ordered lattice within a layer (Fig. 2D) it probably maintains distinct layers in the vertical direction, thus enhancing coherent reflection.

We therefore conclude that each of the strains provides a specific optical fingerprint, which is not only to be attributed to the actual dimensions of the bacteria but mainly to their ability to locally self-organise in a defined lattice. In fact, while the dimensions of WT and M5 were comparable, they displayed a radically different optical response. Moreover, M16 maintained correlation on a longer scale than the WT, indicating that it is possible to improve the regularity of the organisation of living optical structures via genetic manipulation.

Analysis of transposon insertion mutants confirm relation between motility and structural colour

The ability of the bacteria to self-organise into a regular lattice is affected by cell-to-cell communication and motility as suggested by Kientz and co-workers (26). Therefore we isolated mutants with defects in motility on ASWBC and ASWBVLow plates to explore this relationship.

Fig. 4B reports the colony expansion rate (drive by motility but requiring growth) of different strains of the bacteria. By comparing the migration rate of WT and mutants obtained during screening of transposon libraries of IR1 on ASWBC plates, it is evident that gliding motility plays an important role in the organisational capability of the colonies when compared to their visual appearance (Fig. 4 and SI Appendix S8). It was notable that colonies displaying structural colour showed a terraced appearance near the edge, suggestive of ordered layers. In particular, we observed that highly motile bacteria, like the WT and M16, organised on ASWBC plates in long-range periodic structures, while reduced motility strains, such as M17, failed to do so. However, motility alone was insufficient to produce a significant order, as in the case of M5 (Fig. 2).

Mutants with no detectable motility and dull colouration M12, M23, M140, M147 were mapped to the *spr*B (*spr*B23::HiMar, *spr*B140::HiMar, *spr*B147::HiMar, *spr*B150::HiMar) and *spr*F (*spr*F12::HiMar and other isolates) genes; all located within the same gene cluster (Fig. 4C and SI Appendix S3). In *F. johnsoniae*, these *spr* genes formed part of a single operon with two other genes involved in gliding motility, *gld*C and *gld*D. This order of genes is conserved in IR1 (28). It is known that the SprB protein in *F. johnsoniae* is located on the cell surface and is required for motility on agar (29), while the SprF protein is involved in the assembly of SprB on the cell surface and infers a lack of motility of the bacteria on agar (28). Therefore, we conclude that the gliding motility in the IR1 has many core components similar to that of *F. johnsoniae*.

Mutants M6 and M17 have transposon insertions in different loci within the *gldi*A gene (*gldi*A6::HiMar and *gldi*A17::HiMar). This gene was the upstream copy of two closely related genes (*gldi*A and *gldi*B), encoding predicted polypeptides of 55 kDa with 55% identity (Fig. 4D). The *gldi* genes were absent from the genome of *F. johnsoniae* UW101 (30). The *gldi* have no assigned function and are only found in a small number of bacteria, an exception being the rhizosphere *Flavobacterium* F52 (31). F52 possesses a single copy of a *gldi* gene (56% and 59% identity comparing the F52 gene to *gldi*A and *gldi*B respectively) and there was a similar arrangement of these genes between IR1 and F52 (Fig. 4D). The genes immediately flanking *gldi*A and *gldi*B in IR1 were not conserved in F52 and were all related genes known to encode membrane or membrane-associated proteins, a member of the SPFH Flotillin group of proteins known to be involved in lipid binding and a member of the NFED membrane anchored proteins (32) and an EamA family integral membrane protein (33). M6 and M17 also showed a dull colouration (e.g. Fig. 4A and SI Appendix Fig. S8J-L). Despite F52 not previously having been described as structurally coloured, we observed colonies with structural colour on ASWB and ASWBLow agar (SI Appendix Fig. S8C-F). The structural colour of F52 was reduced in a non-spreading mutant 453 with a knockout (KO) of the *gld*J gene, which encodes the GldJ lipoprotein required for motility in *Flavobacteria* (34) (SI Appendix Fig. S8).

In addition, another non-motile and dull mutant of IR1 (M141) was also mapped to a homologue of the *wzx* gene (*wzx*141::HiMar, Fig. 4C), predicted to encode a MATE family protein. Close homologues to the IR1 *wzx* gene were only found in very few flavobacteria with no role described. However, this gene has been implicated in swarming motility mediated by flagella, facilitating wetting agar surfaces to promote migration (35). Taken together, it is clear that mutants with decreased motility affect the formation of structural colour. The involvement of some of these motility genes could have been predicted from studies on other *Flavobacteria* (28–31) whilst the others reported here are novel or with a known function but not previously implicated in gliding motility.

Moreover, we observed the WT structural colouration was lost by mixing the cells in a colony with a sterile inoculation loop but reformed rapidly within 5 to 30 min (Movie S1), which required metabolic energy but not *de novo* protein synthesis (SI Appendix Fig. S9). The motility mutants described above were similarly able to reform colouration, albeit more slowly (30 min to 6 h) and creating a duller colouration than the WT strain, when replated on nutrient agars (SI Appendix Fig. S8G-L). However, unlike the WT, this rearrangement was not possible for non-motile strains M12, M17 and M23 when transferred to agars non-permissive for growth. It is therefore concluded that growth was not required for reforming coloured structures in situations where gliding motility is active and the cell colony was previously structurally coloured. The IR1 colony can therefore be considered a self-organising system only requiring energy and a suitable surface to rapidly reform structural colour.

We conclude that gliding motility is necessary to obtain efficient colony organisation and observe a strong optical response. For mutants defective in gliding, cell growth and division may still facilitate sufficient cell movement and alignment to permit a limited degree of regular packing and colour.

Not only motility genes affect structural colouration

In the genome of the dull but motile mutant M5, a single transposon insertion was found in a gene closely related to the *spo*T gene of *E. coli* (SI Appendix Fig. S2). The SpoT
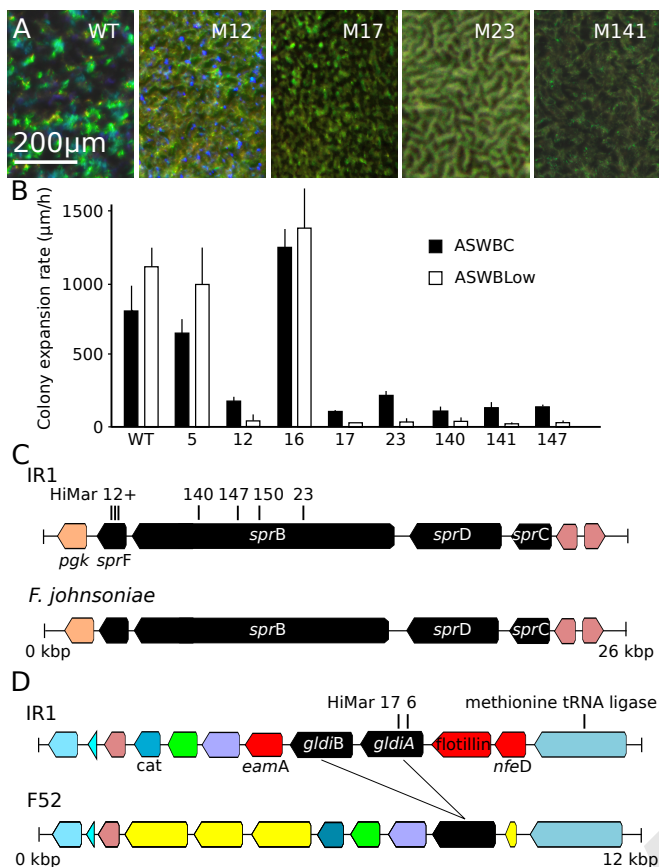
Fig. 4. Phenotyping and mapping of transposon insertions affecting motility and iridescence. A) Comparison of iridescence of WT IR1 and mutants viewed under the microscope and cultured on ASWBC agar overnight at 22 °C. M12-M23 have been colour enhanced since they would otherwise appear black in comparison. B) The rate of colony expansion of the WT and mutant strains quantified on ASWBC and ASWVLow plates. C) Mapping of transposon insertions of mutants 12, 23, 147 and 149 within the *spr*C-F gene cluster of strain IR1, showing close homology with a similar operon from *F. johnsoniae* UW101. D) Mapping of mutants 6 and 17 within the *gldi*A gene of IR1 and comparison with the region of *Flavobacterium* F52 genome that contains homologous gene (black, a single copy in F52 and two in IR1). Genes marked in yellow are only found in this region for F52. Genes in red (*eam*A, a flotillin motif containing gene and *nfe*D) are only found in this region in IR1. Other colours indicate ORFs found in this region in common between the two bacteria, including a putative methionine tRNA ligase upstream and the *cat* chloramphenicol resistance gene downstream.

protein is an enzyme with the capability of degrading guanosine tetraphosphate (ppGpp), the alarmone that triggers a decrease in transcription of many genes (36). In *E. coli* a *spo*T knockout leads to an elevated level of ppGpp. In order to test whether the activation of the stringent response (elevated level of ppGpp) inhibited iridescence, WT IR1 was grown with DL-serine hydroxamate (DLSH), which induces ppGpp synthesis via the inhibition of seryl-tRNA synthetase and the failure to charge the tRNA leading to starvation for that amino acid (37). DLSH was a strong inhibitor of iridescence, but not of gliding. The cells sustained rates of up to 800 mm/h on ASWLow plates, which is similar to the WT. In other words, the effects of DLSH gave a similar phenotype to M5 (*spo*T::HiMar), inhibiting the formation of structural colour. Two independent knockouts (M49, M64) were obtained in a putative *trm*D tRNA methyltransferase (44% identity). Such knockouts completely abolished the structural coloura-

tion whilst allowing growth and motility, suggesting a possible role in the fidelity of translation in regulating structural colour (38).

Moreover, possible interaction of the colonies with plants is suggested by the screening of three mutant strains, M40, M86 and M88. A transposon insertion (M40) into a putative GH3 family gene gave the phenotype of losing colouration faster than the WT (without dying faster). The GH3 family consists of enzymes known to structurally modify plant growth hormones, suggesting a link to the growth of IR1 on macroalgae, the latter are known to produce auxins, benzoates and other hormones. The closest homology was to a GH3.12 containing polypeptide from *Solanum lycopersicum* (tomato), which modifies benzoates with a glutamine residue (39). Whilst the predicted polypeptide was widely distributed in *Flavobacteria*, there is no evidence for the function in this family. In addition, a transposon insertion into a putative endoxylanase (M86 and M88) led to a dull phenotype on ASWBC agar.

Repeated independent transposition events resulted in the highly motile, highly organised colonies described in Fig. 1 and Fig. 2. Mutant 16 (*hyp*A16::HiMar) was typical and analysed in detail. The gene disrupted is one of unknown function, but predicted by domain motifs to encode a SRPBCC deep hydrophobic ligand-binding domain (40). Closely related genes to *hyp*A were widely distributed in the *Flavobacteria*, for which automated annotation indicated a putative transcription factor. However, homology searches outside the *Flavobacteria* and domain searches failed to reveal any support for a role in transcription.

Presence of macroalgae influences the growth of bacteria

As structural colouration by *Flavobacteria* only has been observed on culture media but never in their natural environment, the biological significance of their colouration remains unclear (27). To investigate if the periodic packing responsible of structural colouration can be sustained in a natural environment, we investigated the growth of IR1 strains on different surfaces available in estuarine environments and the effect of natural nutrients as well as in the presence of commonly available algal polymers.

It was found that fucoidan (a sulphated polymer from brown algae) and starch maintained the periodic packing of the WT and could tune the diffraction response towards colours at higher and lower wavelengths. Red, blue and purple appearances were observed in addition to green when growing the WT on ASWBC. The purple/blue colouration was most obvious in young colonies and with high concentrations of starch or fucoidan above 1% (w/v) (see SI Appendix Tables S1 and S2). After 5-8 days at 20 °C on most permissive nutrient agars, including ASWLow plates, colouration was completely lost. Addition of powdered fucoidan within 1 to 2 days of loss of structural colouration caused reordering of the cells of IR1 to allow recovery of structural colour, see Fig. 5B. These observations suggest that the presence of such nutrients is important in the natural environment of IR1 and that the loss of structural colour in ageing colonies is reversible (further screenings are described in Section S1).

IR1 grown under most conditions failed to influence the growth or colouration of a second culture on another agar plate when separated by 1 cm air gap from the second plate (Fig.
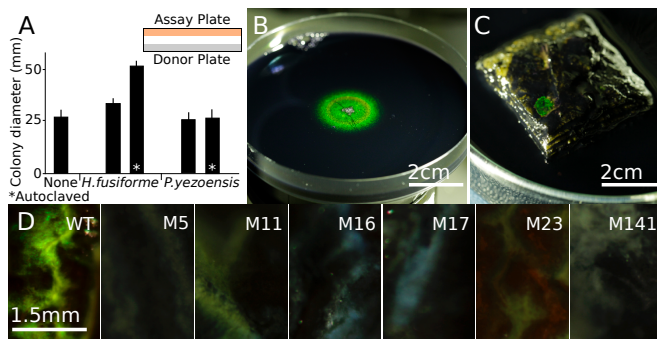
Fig. 5. The effect of growth on algae and algal products directly and indirectly on IR1. A) The effect of exposing IR1 to volatiles from the algae *Pyropia yezoensis* and *Hijikia fusiforme*. An ASWLow plate (Assay Plate) was inoculated in the centre with a 10 μl aliquot containing 10^7 cfu of WT IR1. This was placed facing a second plate (Donor Plate) containing salt agar without algae, or with 10 g of the specified hydrated algae (either autoclaved or not). Plates were sealed with parafilm and incubated for 7 days under humidified conditions. B) Example of fucoidan triggered recovery of structural colour. The entire 9 cm diameter agar plate was spread with IR1, which became intensely green across the whole plate after 24 h and then lost colouration completely after 7 days. Addition of 50 mg of powdered fucoidan to the centre of the plate facilitated recovery of structural colour after 1 day, as shown. C) Wild type IR1 shown growing as a 6 mm diameter iridescent green colony on a 4×4 cm^2 stack of *P. yezoensis* after 18 h at 20 °C. The algae were embedded in agarose with 1% (w/v) KCl and nigrosin. D) Culture of WT and IR1 mutants on 4 mm diameter stalks of *H. fusiforme* after 36 h. Same scale bar.

5A). Exposure to volatiles from IR1 cultured with fucoidan prolonged structural colouration for 3 days. This suggests that the bacteria were releasing influential volatiles from the breakdown of fucoidan. Volatiles from the red algae *Pyropia yezoensis* and brown algae *Hijikia fusiforme* were tested for their effects on the WT strain cultured on ASWB and ASWB-VLow plates. Exposure to *P. yezoensis* had little effect, but on ASWB plates *H. fusiforme* stimulated growth and larger, more coloured colonies. This effect was terminated either by ventilating the cultures or autoclaving the algae (Fig. 5A). Taken together, these experiments suggested IR1 growing on algal products or exposure to brown algae could promote the organisation of other cells of IR1 at a distance of at least 1 cm.

The influence of algae and algal products, combined with the observations that IR1 only formed structural colour on hydrated surfaces exposed to air and that the salinity optimum was 1% (w/v) suggested the possibility that structural colour may form in nature in the estuarine environment. Biotic surfaces likely to be available to IR1 were screened for their ability to support growth of IR1 displaying structural colour. Materials from both animals and macroalgae from estuarine environments were collected. By growing the WT on animal material (fish, crustacea) or rocks coated with microbial biofilms we were not able to observe any effect of structural colouration from the WT after 1 to 14 days. While organisation on most macroalgae was limited, the surface of *Pyropia yezoensis* derived from fresh or dried sources, demonstrated to be a good substrate with strong, green structural colouration forming rapidly 20 min after transfer with the greatest intensity after 8 h and persistence up to 2 days (Fig. 5C). The development of colour was very similar in kinetics and appearance to ASWBC medium containing κ-carrageenan. Structural colouration ranging from green to blue was also observed on the surface of *Hizikia fusiforme* (Fig. 5D). In this case, the colouration appeared after a few hours and persisted

for up to 20 days, which is three times longer than on ASWBC medium where it generally only lasts for a week.

Mutants were screened for their ability to form structurally coloured colonies on *H. fusiforme* (Fig. 5D). The strains M5 (*spo*T5::HiMar) and M17 (*gldi*A17::HiMar) were impaired in colouration on ASWBC plates and did not form structurally coloured colonies on the algal surface. M16 (*hyp*A16::HiMar), despite being intensely coloured on ASWBC agar, was not able to form coloured colonies on the algae. Motility mutants M12 (*spr*F12::HiMar) and M23 (*spr*B23::HiMar) and M141 (*wsx*141::HiMar) were able to form coloured colonies only to a limited extent. These data suggest that the surfaces of red, and particularly brown macroalgae (rich in fucoidan) can be good substrates for the organisation of IR1 to form structurally coloured colonies in nature and that motility assists organisation on the surfaces.

Discussion

We studied the genotype and phenotype relations governing structural colouration in bacteria, showing the possibility to engineer structural colour in a living organism. *Flavobacterium* IR1 showed a formidable capacity and flexibility to organise as a colony, drastically modifying its optical appearance in terms of spectral and angular response under different growth conditions and with genetic modification. We demonstrated that structural colouration of the colonies was linked to motility and other cellular functions including genes with no previously assigned function. Our observations shed light on the biological function of structural colouration in bacteria and suggest an interaction of IR1 with macroalgae. This may relate to photoprotection of bacteria or host, or optimum organisation to degrade biological polymers, with structural colour a secondary consequence.

This presentation of IR1 as a rapidly self-organising system, only requiring competent living cells sustaining a proton motive force and a suitable surface, showcases a highly flexible model organism, which can be used as a future bio-material for photonic applications. As an example, dehydrated and fixed structures composed of bacteria can be engineered for paints and nanotemplates. Moreover, we envision viable pathways for engineering bacteria towards living sensors with intrisic self-healing capabilities. As an example, they can be optimised for changing colouration under external stimuli and interface with other living tissues.

Materials and Methods

Details of the materials and methods are given in SI Appendix. Briefly: strain IR1 (a novel *Flavobacterium* isolated from Rotterdam Harbour, NL) was grown on culture media with salinity matching the location where it was isolated (0.5%-1.5%) or directly on the surface of macroalgae. The IR1 genome was sequenced by Illumina Hi-seq paired-end technology. More than 20,000 colonies from HiMar transposon library were screened for mutants altered in colour, with transposon insertions mapped on the genome as previously described (30). Colonies of IR1 were fixed under conditions which maintained structural colour for electron microscopy. The arrangement of cells in colonies from SEM were measured in ImageJ. Autocorrelation analysis of the SEM images was furthermore performed using in-house computer scripts and presented in SI Appendix. Optical analysis of structural colour was by goniometry

and was performed on live samples using a custom-made goniometer. Analysis of the recorded date relied the grating equation and peak extraction was via in-house computer scripts. Additional data related to this publication is available at the University of Cambridge data repository (doi.org/10.17863/CAM.16794). The genome sequence of IR1 is available from GenBank with accession number NQOT00000000.

1. Kinoshita S (2008) *Structural Colors in the Realm of Nature*. (World Scientific Publishing Company).

2. Kinoshita S, Yoshioka S (2005) Structural colors in nature: The role of regularity and irregularity in the structure. *ChemPhysChem* 6:1442–59.

3. Vukusic P, Sambles JR (2003) Photonic structures in biology. *Nature* 424:852–55.

4. Prum RO, Torres RH (2003) A fourier tool for the analysis of coherent light scattering by bio-optical nanostructures. *Integr. Comp. Biol.* 43:591–602.

5. Wiersma DS (2013) Disordered photonics. *Nat. Photonics* 7:188–96.

6. Vukusic P, Hallam B, Noyes J (2007) Brilliant whiteness in ultrathin beetle scales. *Science* 315:348.

7. Chandler CJ, Wilts BD, Brodie J, Vignolini S (2017) Structural color in marine algae. *Adv. Opt. Mater* 5:1600646.

8. Hahnke RL, Harder J (2013) Phylogenetic diversity of *Flavobacteria* isolated from the north sea on solid media. *Syst Appl Microbiol* 36:497–504.

9. Kientz B, Agogué H, Lavergne C, Marié P, Rosenfeld E (2013) Isolation and distribution of iridescent *Cellulophaga* and other iridescent marine bacteria from the charente-maritime coast, french atlantic. *Syst Appl Microbiol* 36:244–51.

10. Doucet SM, Meadows MG (2009) Iridescence: a functional perspective. *J. Royal Soc. Interface* 6:S115–32.

11. Wilts BD, Michielsen K, Raedt HD, Stavenga DG (2014) Sparkling feather reflections of a bird-of-paradise explained by finite-difference time-domain modeling. *Proc. Natl. Acad. Sci. U.S.A.* 111(12):4363–68.

12. Shi NN, et al. (2015) Keeping cool: Enhanced optical reflection and radiative heat dissipation in saharan silver ants. *Science* 349(6245):298–301.

13. Li L, et al. (2015) A highly conspicuous mineralized composite photonic architecture in the translucent shell of the blue-rayed limpet. *Nat. Commun.* 6(6322):11.

14. Jacobs M, et al. (2016) Photonic multilayer structure of *Begonia* chloroplasts enhances photosynthetic efficiency. *Nat. Plants* 2(16162):6.

15. Whitney HM, et al. (2009) Floral iridescence, produced by diffractive optics, acts as a cue for animal pollinators. *Science* 323:130–3.

16. Whitney HM, Reed A, Rands SA, Chittka L, Glover BJ (2016) Flower iridescence increases object detection in the insect visual system without compromising object identity. *Curr. Biol.* 26:802–8.

17. Ghiradella HT, Butler MW (2009) Many variations on a few themes: a broader look at development of iridescent scales (and feathers). *J. Royal Soc. Interface* 6:S243–51.

18. Prum RO, Dufresne ER, Quinn T, Waters K (2009) Development of colour-producing β-keratin nanostructures in avian feather barbs. *J. Royal Soc. Interface* 6:S253–65.

19. Onelli OD, et al. (2017) Development of structural colour in leaf beetles. *Sci. Rep.* 7(1373).

20. Wilts BD, et al. (2017) Butterfly gyroid nanostructures as a time-frozen glimpse of intracellular membrane development. *Sci. Adv.* 3(4):e1603119.

21. Cuthill IC, et al. (2017) The biology of color. *Science* 357:eaan0221.

22. Shrivastava A, Lele PP, Berg HC (2015) A rotary motor drives *Flavobacterium* gliding. *Curr. Biol.* 25:338–41.

23. McBride MJ (2001) Bacterial gliding motility: Multiple mechanisms for cell movement over surfaces. *Annu. Rev. Microbiol.* 55:49–75.

24. Cousin S, Päuker O, Stackebrandt E (2007) *Flavobacterium aquidurense* sp. nov. and *Flavobacterium hercynium* sp. nov., from a hard-water creek. *Int. J. Syst. Evol. Microbiol.* 57:243–9.

25. Bernardet JF, Nakagawa Y, Holmes B (2002) Proposed minimal standards for describing new taxa of the family *Flavobacteriaceae* and emended description of the family. *Int. J. Syst. Evol. Microbiol.* 52:1049–70.

26. Kientz B, et al. (2012) Glitter-like iridescence within the bacteroidetes especially *Cellulophaga spp.*: Optical properties and correlation with gliding motility. *PLoS One* 7(12):1–12.

27. Kientz B, et al. (2016) A unique self-organization of bacterial sub-communities creates iridescence in cellulophaga lytica colony biofilms. *Sci. Rep.* 6(19906):11.

28. Rhodes RG, Nelson SS, Pochiraju S, McBride MJ (2011) *Flavobacterium johnsoniae sprB* is part of an operon spanning the additional gliding motility genes *sprC*, *sprD*, and *sprF*. *J. Bacteriol.* 193(3):599–610.

29. Nelson SS, Bollampalli S, McBride MJ (2008) Sprb is a cell surface component of the *Flavobacterium johnsoniae* gliding motility machinery. *J. Bacteriol.* 190(8):2851–7.

30. McBride MJ, et al. (2009) Novel features of the polysaccharide-digesting gliding bacterium *Flavobacterium johnsoniae* as revealed by genome sequence analysis. *Appl. Environ. Microbiol.* 75(21):6864–75.

31. Kolton M, et al. (2012) Draft genome sequence of *Flavobacterium* sp. strain f52, isolated from the rhizosphere of bell pepper (*Capsicum annuum* l. cv. maccabi). *J. Bacteriol.* 194(19):5462–3.

32. Hinderhofer M, et al. (2009) Evolution of prokaryotic spfh proteins. *BMC Evol. Biol.* 9:19.

33. Västermark Å, Almén MS, Simmen MW, Fredriksson R, Schiöth HB (2011) Functional specialization in nucleotide sugar transporters occurred through differentiation of the gene cluster eama (duf6) before the radiation of *Viridiplantae*. *BMC Evol. Biol.* 11:123.

34. Kolton M, Frenkel O, Elad Y, Cytryn E (2014) Potential role of flavobacterial gliding-motility and type ix secretion system complex in root colonization and plant defense. *MPMI* 27(9):1005–1013.

35. Toguchi A, Siano M, Burkart M, Harshey RM (2000) Genetics of swarming motility in *Salmonella enterica* serovar typhimurium: Critical role for lipopolysaccharide. *J. Bacteriol.* 182(22):6308–21.

36. Laffler T, Gallant J (1974) *spot*, a new genetic locus involved in the stringent response in e. coli. *Cell* 1(1):27–30.

37. Christensen SK, Mikkelsen M, Pedersen K, Gerdes K (2001) Rele, a global inhibitor of translation, is activated during nutritional stress. *Proc. Natl. Acad. Sci. U.S.A.* 98(25):14328–33.

38. Hori H (2014) Methylated nucleosides in trna and trna methyltransferases. *Front. Genet.* 5(144):1–26.

39. Westfall CS, Herrmann J, Chen Q, Wang S, Jez JM (2010) Modulating plant hormones by enzyme action: The gh3 family of acyl acid amido synthetases. *Plant Signal Behav.* 5(12):1607–12.

40. Iyer LM, Koonin EV, Aravind L (2001) Adaptations of the helix-grip fold for ligand binding and catalysis in the start domain superfamily. *Proteins: Struct., Funct., Genet.* 43:134–44.